RSC Sustainability

ROYAL SOCIETY OF CHEMISTRY

PAPER

View Article Online
View Journal | View Issue

Cite this: *RSC Sustainability*, 2025, **3**, 1516

Using ultrasonic oil–water nano-emulsions to purify lithium-ion battery black mass†

Chunhong Lei, Karl S. Ryder, Andrew P. Abbott and Jake M. Yang *

Long-loop recycling of spent lithium-ion batteries is neither sustainable nor economical at scale. In the absence of design-to-recycle initiatives taken up by cell manufacturers, even for batteries produced today, all-in-one shredding processes are the only practical option to achieve circularity of critical materials. Shredding lithium-ion batteries ultimately produces 'black mass' – a low-value commodity comprising a mixture of graphite from the anode and lithium metal oxides from the cathode. Recovery of valuable metals such as cobalt and nickel from black mass using energy-intensive pyro- and hydro-metallurgy processes inevitably destroys the crystalline structure of lithium metal oxides and thus requires further resynthesis of battery material upon isolation and purification. This study presents an efficient process for direct separation of graphite and lithium metal oxides from numerous sources of black mass by utilizing a meta-stable oil-in-water emulsion. The purification of black mass is facilitated by one minute of high-power ultrasonic agitation followed by sieve separation, whereby the ultrasonic process enabling purification requires *ca.* 1% of the energy for heat removal of the binder. The separation exploits the disparity in hydrophobicity between graphite and lithium metal oxides, with ultrasonic energy enhancing the efficacy of the process to allow separation of cathode and anode counterparts with purity as high as 96% within minutes of operation. This innovative approach offers a promising solution for short-loop recycling of lithium-ion battery black mass.

Received 5th December 2024
Accepted 30th January 2025

DOI: 10.1039/d4su00771a

rsc.li/rscsus

Sustainability spotlight

Amidst the global rise in electrifying transportation to meet net zero goals, there are over 10 billion active mobile phones, laptops and tablets worldwide powered by various lithium battery chemistries waiting to be recycled when they reach their end-of-life. However, the lack of regulations means lithium-ion battery packs are not designed for recycling. Recovery of valuable metals from recycled lithium-ion battery black mass involves smelting and/or the use of a highly corrosive leachate to re-extract valuable metals. In this work, we circumvent the aforementioned long-loop material recovery *via* direct purification of black mass using 1% vegetable oil-in-water and short bursts of ultrasonic agitation. This low-cost separation approach enables short-loop recycling of lithium-ion batteries.

The widespread adoption of lithium-ion batteries (LIBs) in energy storage systems and powering transportation is a global effort to slow climate change *via* sustainable technologies. In addition to the estimated 40 million electric vehicles (EVs) globally, there are approximately 10 billion active mobile phones, laptops and tablets worldwide,[1] all powered by various LIB chemistries.[2] Demand for LIBs is increasing rapidly driven, in part, by legislation to decarbonise transport. In the UK alone, it has been estimated that a stockpile of *ca.* 70 000–106 000 units of obsolete end-of-first-life EV batteries are waiting to be recycled in 2025,[3] and by 2028, 16 650 tonnes of EV batteries will need to be recycled.[4] For LIBs to become a sustainable technology, the recycling capacity of LIBs will need to scale with the rate of production before batteries produced today reach their end-of-life, which is typically 8–10 years after market entry.[3,5]

The major challenge facing all LIB recyclers is the low profit-margin for recycling resulting from the complex pack design. Battery pack dismantling is labour-intensive and hazardous. For recycling LIBs to be profitable with current processing methods, the operational cost for recyclers needs to be within $2–6 per kilogram of the spent battery, without accounting for labour costs and assuming a gate fee-free process.[6] The roadmap for lithium-ion and other battery technologies to achieve a sustainable circular economy is not without challenges, as detailed elsewhere.[7]

LIB recycling usually starts by shredding cells to facilitate the removal of inactive constituents such as copper, aluminium, and polymer separators *via* sieving, winnowing, magnetic separation, and other methods. This processing leaves behind the active components—graphite and lithium metal oxides—forming what is known as 'black mass'.[8] Processing steps are illustrated in Fig. 1a. The quality and thus the value of black

School of Chemistry, University of Leicester, Leicester LE1 7RH, UK. E-mail: jake.yang@leicester.ac.uk

† Electronic supplementary information (ESI) available. See DOI: https://doi.org/10.1039/d4su00771a

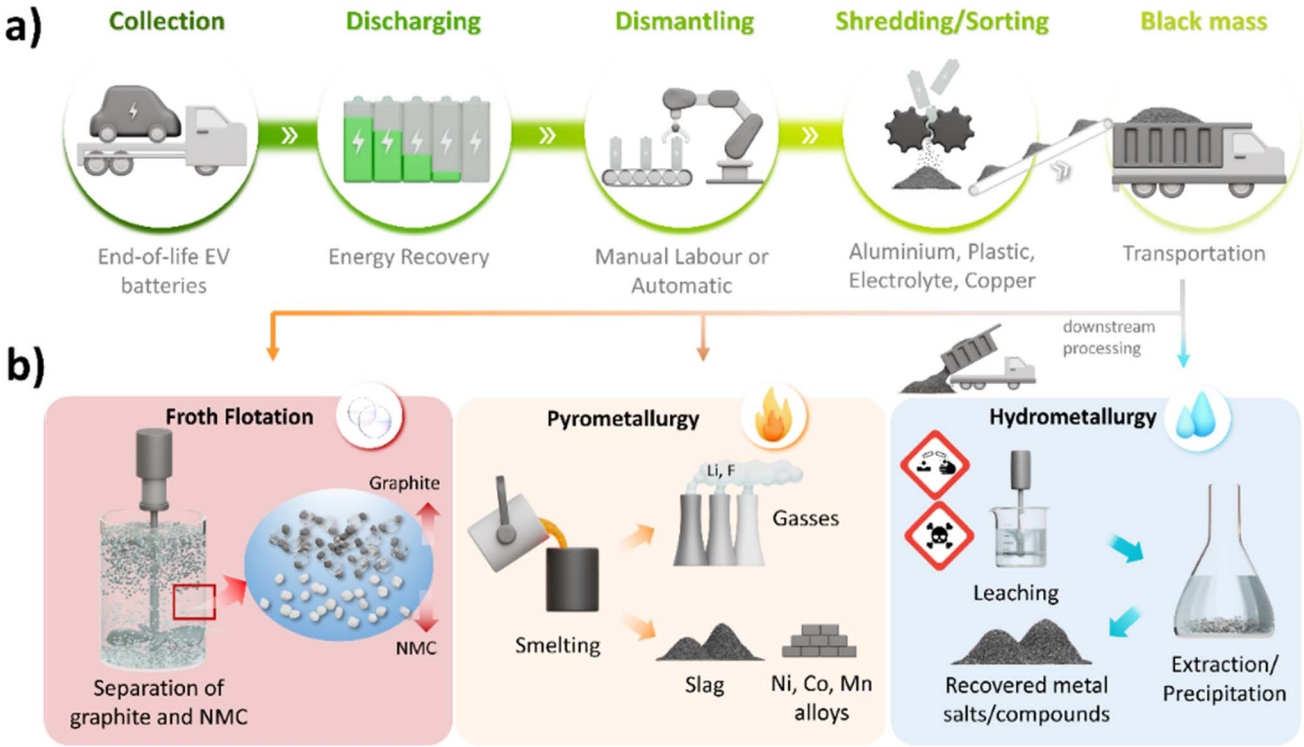

Fig. 1 Typical recycling pipeline for end-of-life EVs. (a) Shredding process of an end-of-life EV involving transportation, discharging and dismantling of battery cells from packs. (b) Subsequent processing of black mass with froth flotation, pyrometallurgy and hydrometallurgy.

mass at the end of a typical recycling pipeline is highly dependent on the purity of black mass and the overall nickel and cobalt content. Black mass is usually sold as a low-cost commodity to hydrometallurgical downstream processes, as shown in Fig. 1b, where valuable metals are reprocessed by either pyrolytically burning off the graphite or dissolving the lithium metal oxide to eventually recover a mixed metal alloy containing Ni, Cu and Co or metal leachates.[9,10] The cathode active material crystallinity is destroyed during the black-mass purification process so further synthesis steps are required to regenerate pristine lithium metal oxides of choice. The challenge for shredders and recyclers is to produce single active battery components by purification of black mass so as to facilitate a direct, short-loop recycling process where the components can be re-used, with little or zero further processing depending on the state of provenance, in the battery manufacturing processes.[7,11]

Direct recycling[12–16] is a newly emerging initiative aimed at recycling LIBs by recovering valuable components (*e.g.* lithium metal oxides and graphite) without compromising or destroying the material's crystal structure. Such processes are usually greener, lower cost and minimize the use of hazardous chemicals, as compared to pyrometallurgy and hydrometallurgy, thus bolstering the sustainability and profitability of battery recycling initiatives. Froth flotation is an example of a direct recycling method, adapted from mineral separation, that could selectively separate graphite from lithium metal oxide particles based on the hydrophobicity and wettability difference between these two materials.[8,17–19] This method yields medium to high purity materials (50 to 95%), depending on the degree of removal of the cathode binder (PVDF).[20,21] The method, although promising, suffers from drawbacks as it necessitates the use of costly frother and collector compounds as well as being time-consuming.[18,22] Moreover, froth flotation is susceptible to issues such as entrainment and entrapment, further diminishing the purity of the desired minerals.[23]

Ultrasonication has emerged as an effective and environmentally friendly method for preparing oil-in-water emulsions as demonstrated by its successful application in the food industry.[24,25] Through ultrasound cavitation, shear forces disrupt oil macro-drops in water, transforming them into nano-droplets with a narrow size distribution.[26,27] In this study, we employ pulverized oil droplets in water without surfactant additives to selectively capture graphite in recycled LIB black mass powder. This method enhances the purity and thus increases the value of the black mass without compromising the crystal structure of the cathode materials. Compared to the surfactants used in froth flotations, the use of oil droplets—whether derived from vegetable oil or minerals oil—presents a cost-effective and readily scalable alternative to short-loop recycling lithium-ion batteries.

Experimental

Oil-in-water emulsions

One volume percent (v/v%) of vegetable oil (Rapeseed Oil (100%), Morrisons, UK) or kerosene (reagent grade, Sigma-Aldrich) was added to 60 mL of deionized (DI) water. Using an

ultrasonicator (model: 1.25DCXa20-V, operating at 20 kHz, maximum power 1250 watts, with a 20 mm diameter cylinder sonotrode), the oil was pulverized with the ultrasonic horn immersed in the oil–water biphasic solution. The power consumption of the ultrasonic horn was set to 30% of peak power (375 watts) unless otherwise stated. The oil and water mixture was subjected to insonation for one minute. During this period, the immiscible oil and water biphasic system turns 'milky' in appearance and the resultant colloidal oil-in-water suspension is found to be kinetically stable for at least two weeks. The size distribution of the resulting oil droplets was analysed using a dynamic light scattering machine (Zetasizer Nano-S, Malvern Instruments).

Black mass blends

The work investigates the separation of three different black mass blends obtained from various sources: a binder-free black mass blend comprised of commercial grade NMC622 and graphite, a black mass delaminated from an end-of-life Nissan Leaf EV (first generation, 2010), and a commercial black mass blend with unknown battery chemistry. The binder-free black mass blend consisting of commercial grade NMC622 and spherical graphite (Imerys Graphite & Carbon) was mixed in a 2 : 1 weight ratio. The Nissan Leaf black mass was prepared by blending delaminated cathode (LMO/NMC) and anode graphite powders in a 2 : 1 weight ratio.

Two grams of black mass were added to the 60 mL oil-in-water emulsion solution followed by a further minute of insonation treatment at 375 watts of ultrasonic operation power. After insonation, the resulting solution contained dispersed particles and oily lumps of congregated particles. A sieve with a 200 μm aperture was used to separate the oil lumps from the dispersed particles. The retentate and the filtrate, after rinsing off oil followed by subsequent drying, were then analysed using scanning electron microscopy (SEM) with an FEI Quanta 650 FEGSEM. A critical minimum threshold of 0.5–1.0 v/v% of vegetable oil was found to be needed to achieve high purity separation of graphite particles from black mass.

The purity of black mass and filtrates separated after the o/w emulsion processes was determined *via* pyrolysis of carbonaceous materials at 850 °C for 3 hours (Lenton Chamber Furnace, thermostated using a Eurotherm 3216 temperature controller). Assuming all carbonaceous materials were fully combusted at 850 °C, the mass of the residue weight was used to infer the purity of the substance post o/w separation.

After the proof-of-concept separation using 2 g of black mass, the work progressed to use the same setup to separate 40 g of commercial black mass. This, however, requires a small tweak in the parameters to optimise separation purity since the size of the ultrasonic horn is not readily scaleable. The revised conditions include an increase of ultrasonic power to 1000 W, a higher black mass loading (40 g in 800 mL of o/w emulsion) and a slightly decreased oil content (0.5 v/v%). The ultrasonic duration of one minute was unaltered from the lab-scale 2 g separation procedure. The results of the 40 g scale-up separation are shown in Fig. S5† and discussed in the main text.

Microscope imaging

Bright-field and fluorescence images of the oil–graphite conglomerate were captured using an epi-fluorescence microscope (BX51M, Olympus) using a 40× objective (LUMPlanFI, 0.80 W, Olympus). Fluorescence image of Nile red in vegetable oil was imaged using the following light source and filters: excitation (λ_{ex} = 490 ± 7 nm, pE-4000, CoolLED), dichromic filter (MD515, Thorlabs) and a long pass emission filter (>590 nm). Image acquisition was provided by a Photometrics Prime sCMOS camera (Teledyne Photometrics), providing 16-bit images with 4-megapixel resolution.

Results

Oil-in-water nano-emulsions

Oil-in-water (o/w) nano-emulsions, without the addition of surfactants, were formed through one minute of insonation of 1 wt% vegetable oil-in-water using a high-power sonohorn as illustrated in Fig. 2a. The resultant mixture exhibits an opaque 'milk-like' appearance which is stable for weeks in ambient conditions. Dynamic light scattering, shown in Fig. 2b, reveals o/w emulsions with a narrow size distribution of 200–400 nm size depending on the oil used. The minor difference between o/w emulsions formed from vegetable oil and kerosene is that the kerosene o/w emulsions float to the top of the solution faster than the vegetable oil emulsions due to their lower density, 0.80 g cm^{-3} *vs.* 0.92 g cm^{-3}, respectively. The formation of oil droplets in water after the minute of insonation treatment is shown by transmission light and fluorescence microscope images in Fig. 2d and e, respectively. Fig. 2e shows a fluorescence image of Nile red, an oil-soluble and water-insoluble dye added to the oil-phase prior to the formation of the o/w emulsion.

Separation of pristine, binder-free graphite and NMC622 blend

Upon pouring the o/w emulsion into a pristine blend of black mass comprising virgin NMC622 and graphite (2 : 1 wt% ratio), distinct behaviours are observed due to the inherent hydrophobicity properties of the blended material. Graphite particles, being hydrophobic, were found to float to the surface of the o/w solution, while NMC622 particles, being hydrophilic and denser than water, tend to settle at the bottom, as can be seen in Fig. 2e and f. In the absence of ultrasound agitation, a minority of the NMC622 particles were found to be floating within the graphite aggregate, and the graphite particles can be entrapped within the sediment containing mostly NMC622 at the bottom of the solution. However, with a further minute of vigorous agitation using ultrasound, the resultant particle mixtures were seen to fully separate into two parts *via* sieve filtration: the flocculated lump (mainly graphite), which floated at the top of the solution, and the sediment (mainly NMC622), as illustrated schematically in Fig. 3a. The oil–wetted graphite conglomerate, shown in Fig. 3h, is larger than the sieve size of 100 μm thus allowing sieve filtration from unaltered NMC particles. The upper image of the graphite conglomerate shown in Fig. 3h is a bright-field

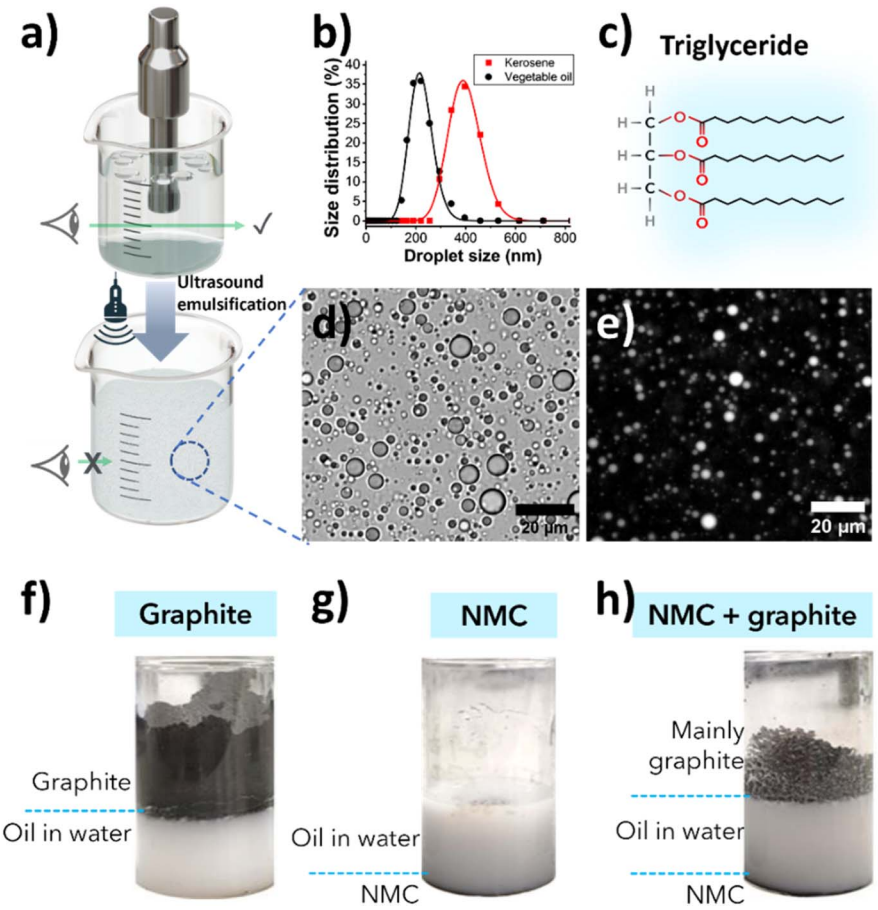

Fig. 2 Ultrasound emulsification of 1% oil-in-water. (a) Illustration of an opaque o/w emulsion formed after one minute of insonation. (b) Size distribution of vegetable oil and kerosene o/w emulsions measured *via* dynamic light scattering. (c) Chemical structure of a triglyceride. (d) Transmission light microscope image of a vegetable o/w emulsion formed after 1 minute of insonation. (e) Fluorescence image of oil-soluble Nile red dye where 1 mM of the dye was pre-dissolved in the oil phase prior to insonation in water as described in (a). The vegetable o/w emulsion was added to (f) graphite, (g) NMC particles and (h) a blend of graphite and NMC without mechanical stirring or agitation.

image whereas the lower image shows fluorescence of the oil, which contains 1 mM Nile red pre-dissolved in the oil phase. Fig. S1† shows transmission light and fluorescence image of a larger oil–graphite conglomerate formed under the same conditions. Fig. 3b and d are macroscale images of the retentate and filtrate obtained after sieve filtration, respectively. Fig. 3c and e show backscattering SEM images of the retentate and filtrate after drying. Graphite particles are discernible as dark, 'potato-shaped' entities, while NMC622 particles manifest as bright, round shapes, owing to the heavier metal elements in comparison to carbon. The separated graphite and NMC622 provides a direct comparison to SEM images of the pristine black mass blend, shown in Fig. 3f. Combustion of the filtrate (at 850 °C for 3 h) obtained after o/w separation reveals a 98.2% purity of NMC particles, assuming that all graphite is removed as CO_2(g) during the pyrolysis step.[28] Fig. S2a and b† show SEM images of the filtrate and retentate over a larger viewing area which unambiguously shows that the purity of separation is consistently uniform throughout the sample. This is not unreasonable since direct pyrolysis of the pristine blend, Fig. 3g, results in a solid residue with weight that is fully consistent with the 2 : 1 weight ratio of the NMC : graphite blend. Separation of the pristine black mass blend was also conducted similarly *via* kerosene emulsions instead of vegetable oil but the separation purity is lower than that of vegetable oil as can be inferred from SEM images shown in Fig. S2.†

Separation of black mass recycled from spent LIBs

The efficiency of o/w separation of two different commercial black mass blends obtained from end-of-life first generation EVs, a Nissan Leaf (UK) and a commercial mixed blend, were examined. First, as illustrated schematically in Fig. 4a, 500 °C heat pre-treatment[29] of commercial black mass was carried out for one hour to remove the binders prior to the o/w emulsion separation. SEM images show black mass obtained from disassembled Nissan Leaf cells, with NCA/LMO battery chemistry, and a commercially available black mass where precise battery chemistries of the blended material were not stated. SEM/EDX analyses of the commercial black mass blend, shown in Fig. S3,† reveal the presence of Ni, Mn and Co, and the absence of Fe and P, showing it came predominantly from NMC batteries. Fig. 4b and c show SEM images of the retentate and filtrate of these two blends after the o/w emulsion separation.

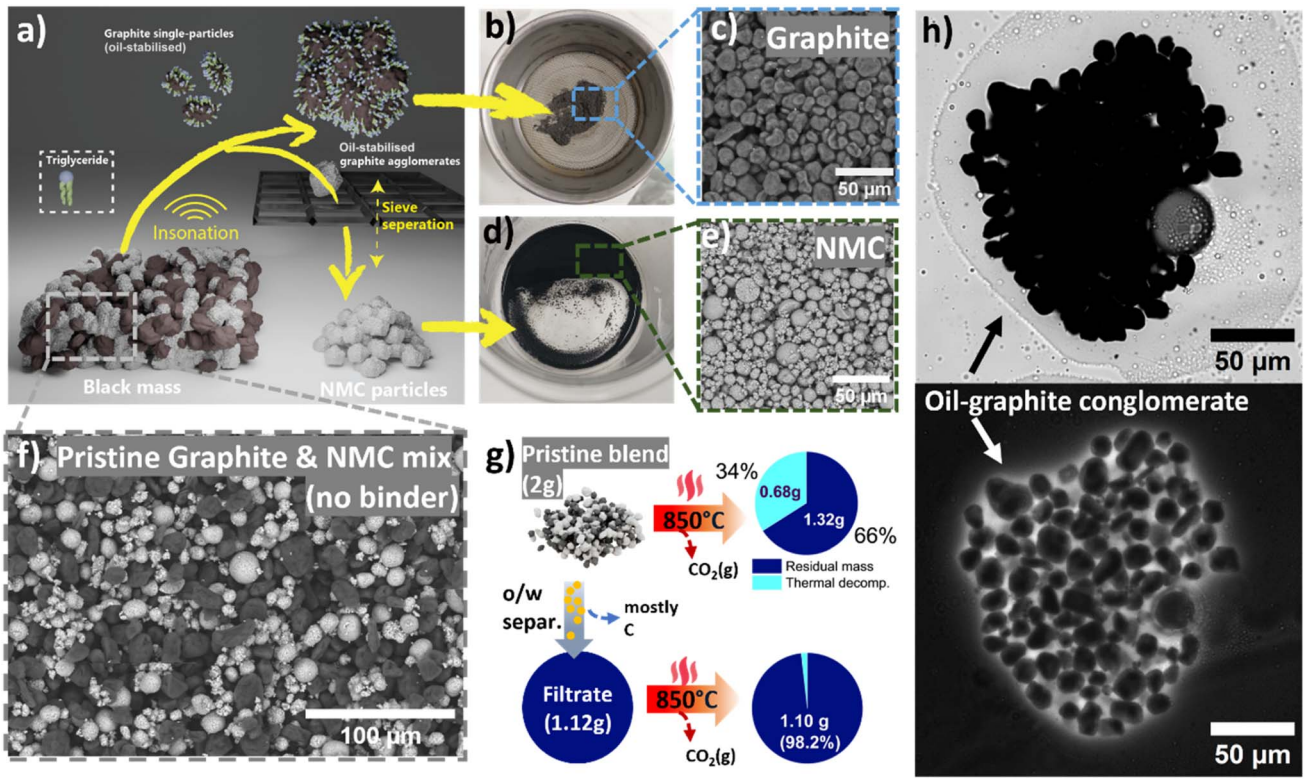

Fig. 3 Separation of pristine, binder-free black mass blend consisting of virgin NMC622 and graphite mixed in a 2 : 1 weight ratio. (a) Schematic of the ultra-sound assisted separation process of black-mass blend using 1% vegetable oil. After one minute of insonation of black mass with vegetable o/w emulsion the resultant mixture was sieve filtered (pore size = 100 μm) to give (b) a retentate and (d) filtrate. (c and e) SEM images of the retentate and filtrate once dried after water and isopropanol washing steps, respectively. (f) SEM image of the pristine black mass blend. (g) Two grams of the pristine black mass blend were treated at 850 °C for 3 h. The resultant solid residue was 1.32 g, which is fully consistent with the 2 : 1 weight ratio of the NMC622 : graphite blend suggesting that all graphite has undergone thermal decomposition in this process. The same pyrolysis treatment was conducted for the filtrate. (h) Optical microscopy images showing a graphite agglomerate after one minute of insonation with 1% vegetable o/w emulsion. The upper image was taken under bright-field and the lower image shows the fluorescence of 1 mM Nile red (λ_{ex} = 490 ± 7 nm and λ_{em} = 560 ± 10 nm), an aqueous insoluble dye pre-dissolved in the oil phase.

Further, direct pyrolysis analysis (850 °C, 3 h) of the filtrate isolated from the commercial black mass reveals a 3.4 wt% mass loss after the heat treatment. From this we infer the filtrate contains cathode active material(s) (CAMs) with 96.6% purity, assuming that all carbonaceous materials are pyrolyzed during the process. This high purity of separation is fully consistent with SEM images as shown in Fig. 4b and c. Furthermore, Fig. S4† shows complementary SEM images of the retentate and filtrate obtained from the two commercial black mass blends over a larger viewing widow.

Discussion

Emulsions are usually only thermodynamically stable when surfactants are used. Ultrasound emulsification of vegetable oil-in-water and, separately, kerosene in water results in an emulsion suspension that is observed to be stable over 2 weeks in the absence of surfactants. This apparent stability of surfactant-free o/w emulsions can be, in part, explained by Stokes' law[30] which governs particle settling or rising velocities:

$$v = \frac{g(\rho_p - \rho_f)d^2}{18\mu} \quad (1)$$

where v is the particle (or droplet) rising or settling velocity, g is the gravitational constant, μ is the dynamic viscosity of water, r_p and r_s are the densities of the particle (or droplet) and water, respectively, and d is the diameter of the particle. According to Stokes' law, the stability of the emulsion solution is partially explained by the slow rising motion of sub-micron sized o/w emulsions. Approximately 14 days are required for the 400 nm sized o/w emulsion to rise by a height of 1 cm in the absence of convection. Therefore, on a macroscopic level, the emulsion is stable against creaming over the observation period, which is fully consistent with experimental observations. On a microscopic level, interestingly, micro- and nano-vegetable oil emulsions in apparent 'contact' with each other were not observed to coalesce over tens of seconds (Online ESI Movie†). It was suggested that the thin water film between two non-coalescing oil droplets, stabilised by high numbers of hydrogen bonding, is prohibiting the surfactant-free oil droplets from coalescing.[31,32] Furthermore, the size of oil droplets formed under ultrasound emulsification is found to be consistent with theory which correlates the size of oil particles with the ultrasound power and cross-section area of the ultrasound horn.[33] This relationship allows optimisation of ultrasonic parameters to achieve the

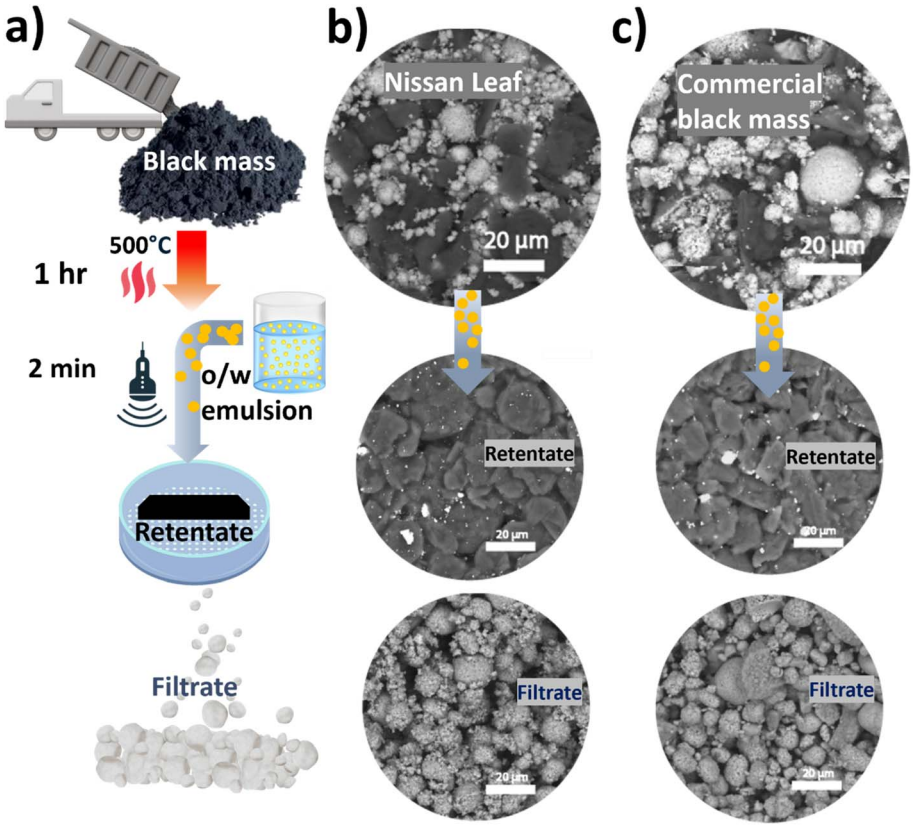

Fig. 4 Oil-in-water purification of two grams of commercial black mass. (a) Purification of commercial black-mass includes a 500 °C heat pre-treatment for one hour to first remove the binder, followed by one minute of ultrasound agitation of the black mass mixture with the o/w emulsion. The oil–graphite conglomerate is then separated from CAM by sieve filtration. (b and c) Backscattering SEM images of black mass from a Nissan Leaf and a commercial black mass blend, respectively.

desired droplet size for emulsion stability and fine-tuning of the separation process.

The surface of graphite, although hydrophobic in nature, is negatively charged as evidenced by zeta potentials reported in the literature.[34] After insonation agitation of graphite in o/w emulsions, the meta-stable oil droplets were found to selectively wet the graphite surface, as evidenced unambiguously by the fluorescence of oil-soluble and water-insoluble Nile red within the conglomerate of graphite particles, shown in Fig. 3h and S1b.† The wetting of the graphite surface with oil overcomes electrostatic repulsion, so as to allow the attractive van der Waals forces to dominate resulting in the formation of large oil–graphite conglomerates during ultrasound agitation. The physicochemical origins of these two opposing forces and how their interplay underpins the kinetic stability of most colloidal systems are described by the DVLO theory which is widely available in most Chemistry undergraduate texts.[35,36] In contrast to the graphite particles, NMC622 particles remain unperturbed in the oil suspension solution due to their hydrophilic nature; the oil nanoemulsions were not found to adhere to the NMC particles, allowing them to remain as individual micron-sized entities with can be separated easily from the oil–graphite conglomerates *via* sieve filtration. Pyrolysis analysis of the filtrate reveals near pure NMC622 (98.2%) was recovered from the pristine 2 : 1 NMC/graphite black mass blend by the o/w separation process.

Commercial black mass, different to the pristine black mass blend, contains a polymeric binder such as PVDF which is used to bind CAMs onto the aluminium current collector in real battery cells to ensure structural integrity of the cathode (and anode) as the battery undergoes charging and discharging cycles. It was found that binder removal was necessary to separate commercial black mass into CAMs and graphite using o/w emulsion. PVDF is, similar to graphite, hydrophobic in nature. PVDF-coated CAMs exhibit similar wetting behaviour to that seen on graphite surfaces and PVDF thus preventing effective separation of CAMs from graphite. This is an issue also reported in froth flotation processes. Other than thermal decomposition treatment, binder removal can be achieved *via* hydrothermal treatment in basic solution,[37] and dissolution with organic solvents such as NMP or greener alternatives like DMSO[38] and acetone at elevated temperatures or pressures.[39] After heat pre-treatment, two commercial black mass blends were successfully separated into highly pure graphite and CAMs within minutes of insonation with a 1% vegetable o/w emulsion, as illustrated in Fig. 4. Purity of the filtrate isolated from commercial black mass is 96.6%, assuming all carbonaceous materials (3.4%) such as graphite and PVDF are burnt off over the three hours of 850 °C heat treatment.

Here, o/w emulsions of three black mass sources have successfully been separated into high purity components on a two-gram scale. Fig. S5† shows an upscale separation of 40 g of commercial black mass using 800 mL of 0.5% o/w emulsion. The retentate and filtrate obtained after sieving, rinsing off the oil residue, and drying were 8.1 g and 29.6 g, respectively. Upon heating the cathode-rich filtrate obtained after o/w emulsion separation for three hours at 850 °C, a mass loss of 13.5% was recorded. The mass loss is assumed to be carbonaceous impurities appearing in the filtrate as discussed above. On the other hand, pyrolysis of the retentate obtained after o/w emulsion separation, which is graphite-rich, resulted in an 80% mass loss. The remaining 20% of the incombustible solids in the retentate were likely to be a combination of lithium metal oxide and dust/sand collated during the battery shredding and black mass collection process. While the purity of separation at scale could be further optimised by changing parameters such as insonation time and varying the % of oil in the o/w emulsion, it is useful to instead compare and contrast the energy consumption of the o/w separation process as compared to, for example, direct incineration of carbonaceous compounds at elevated temperature (850 °C) to isolate CAMs from black mass. Table S1† shows the energy consumed during the separation of 40 g of black mass using an o/w emulsion. Most notably, the 2 minutes of ultrasonic processing used merely 5.6 W h of energy as compared to the cost of heating, which is 453 W h and 821 W h to maintain the oven at 500 °C to remove the battery binder and 850 °C to burn off carbonaceous compounds, respectively.

Conclusions

Vegetable oil, water and ultrasound were found to efficiently separate graphite from lithium metal oxides from heat pre-treated black mass obtained from various sources within minutes of operation. In the absence of surfactants, ultrasound-generated oil-in-water nano-emulsions are kinetically stable over weeks of observation. Graphite particles, which are hydrophobic and oleophilic in nature, are selectively wet by these meta-stable o/w emulsions to overcome the electrostatic repulsion, allowing van der Waals attractions to dominate. These large oil–graphite conglomerates, hundreds of microns in size, can be easily sieved away to result in a high purity of cathode materials in the filtrate (96.6%). We have demonstrated success in the separation of three different sources of black mass. Most importantly, the use of ultrasound to generate o/w nanoemulsions required for the separation process and for the further minute of ultrasound agitation costs only *ca.* 1% of total energy consumption. The remaining 99% is associated with the heat removal of the PVDF binder at 500 °C. Nevertheless, the total cost for o/w separation of black mass including the heat pre-treatment step, based on laboratory-based 40 g scale-up, is approximately 44% lower in energy consumption as compared to direct incineration of black mass at 850 °C for one hour. It is clear that o/w black mass purification is not only much less energy intensive and involves shorter steps compared to pyrometallurgy processes, which require subsequent resynthesis steps, but is also greener because graphite is filtered away as opposed to incinerated which releases greenhouse gases.

We foresee this scientific discovery will facilitate a rapid separation of black mass into highly pure cathode and anode counterparts, providing a novel route to direct short-loop recycling of lithium-ion batteries. Further, the removal of binders such as PVDF remains a challenge for all LIB recycling routes. Innovations of water-soluble battery binders provide the key missing puzzle to cut the energy consumption associated with o/w purification of black mass by 99%.

Data availability

The data supporting this article have been included as part of the ESI.†

Author contributions

CL: writing – original draft, investigation (lead), formal analysis, validation, methodology. KSR: funding acquisition, writing – review & editing. APA: funding acquisition, writing – review & editing, supervision, conceptualization. JY: writing – original draft, investigation, writing – review & editing, supervision, visualization.

Conflicts of interest

The authors have filed a patent based on this work with the Leicester Innovation Hub.

Acknowledgements

The authors thank the Faraday Institution (Faraday Institution grant code FIRG027, project website **https://relib.org.uk**), Innovate UK for funding under the Reblend project (10043366), and the SonoCat project (grant EP/W018632/1), UK Engineering and Physical Sciences Research Council (EPSRC), for funding this work.

References

1 *Digital media and wireless communications in developing nations: agriculture, education, and the economic sector*, ed. M. R. Goyal and E. Eilu, CRC Press, 2019.
2 A. A. Akcil, *Critical and rare earth elements: recovery from secondary resources*, CRC Press, 2019.
3 J. P. Skeete, P. Wells, X. Dong, O. Heidrich and G. Harper, *Energy Res. Soc. Sci.*, 2020, **69**, 101581.
4 L. Brückner, J. Frank and T. Elwert, *Metals*, 2020, **10**, 1107.
5 A. Zanoletti, E. Carena, C. Ferrara, E. Bontempi and O. S. Burheim, *Batteries*, 2024, **10**, 38.
6 D. Thompson, C. Hyde, J. M. Hartley, A. P. Abbott, P. A. Anderson and G. D. Harper, *Resour. Conserv. Recycl.*, 2021, **175**, 105741.

7 G. D. Harper, E. Kendrick, P. A. Anderson, W. Mrozik, P. Christensen, S. Lambert, D. Greenwood, P. K. Das, M. Ahmeid and Z. Milojevic, *J. Phys.: Energy*, 2023, **5**, 021501.
8 A. Vanderbruggen, A. Salces, A. Ferreira, M. Rudolph and R. Serna-Guerrero, *Minerals*, 2022, **12**, 72.
9 B. Makuza, Q. Tian, X. Guo, K. Chattopadhyay and D. Yu, *J. Power Sources*, 2021, **491**, 229622.
10 J. C.-Y. Jung, P.-C. Sui and J. Zhang, *J. Energy Storage*, 2021, **35**, 102217.
11 S. E. Sloop, J. E. Trevey, L. Gaines, M. M. Lerner and W. Xu, *ECS Trans.*, 2018, **85**, 397.
12 A. K. Vinayak, Z. Xu, G. Li and X. Wang, *Renewables*, 2023, **1**, 294–315.
13 A. A. Pavlovskii, K. Pushnitsa, A. Kosenko, P. Novikov and A. A. Popovich, *Inorganics*, 2022, **10**, 141.
14 M. Y. Guan, P. Lou, G. H. Xu, K. Y. Zhou, W. X. Zhang and Q. Cheng, *Ionics*, 2023, **29**, 97–103.
15 K. Park, J. L. Yu, J. Coyle, Q. Dai, S. Frisco, M. Zhou and A. Burrell, *ACS Sustain. Chem. Eng.*, 2021, **9**, 8214–8221.
16 P. P. Xu, D. H. S. Tan, B. L. Jiao, H. P. Gao, X. L. Yu and Z. Chen, *Adv. Funct. Mater.*, 2023, **33**, 2213168.
17 Y. He, T. Zhang, F. Wang, G. Zhang, W. Zhang and J. Wang, *J. Clean. Prod.*, 2017, **143**, 319–325.
18 S. D. Barma, P. K. Baskey, D. S. Rao and S. N. Sahu, *Ultrason. Sonochem.*, 2019, **56**, 386–396.
19 X. Ma, P. Ge, L. Wang, W. Sun, Y. Bu, M. Sun and Y. Yang, *Molecules*, 2023, **28**, 4081.
20 G. Zhang, Y. He, H. Wang, Y. Feng, W. Xie and X. Zhu, *J. Clean. Prod.*, 2019, **231**, 1418–1427.
21 S. Nazari, A. B. Vakylabad, K. Asgari, J. Li, H. Khoshdast, Y. He and A. Hassanzadeh, *J. Energy Storage*, 2024, **84**, 110702.
22 R. Golmohammadzadeh, F. Faraji, B. Jong, C. Pozo-Gonzalo and P. C. Banerjee, *Renew. Sustain. Energy Rev.*, 2022, **159**, 112202.
23 L. WAng, Y. Peng, K. Runge and D. Bradshaw, *Miner. Eng.*, 2015, **70**, 77–91.
24 Y. J. Li and D. Xiang, *PLoS One*, 2019, **14**, e0213189.
25 Q. Q. Fu, H. B. Shi, L. Zhou, P. P. Li and R. R. Wang, *Int. J. Food Sci. Technol.*, 2022, **57**, 2523–2534.
26 M. Sivakumar, S. Y. Tang and K. W. Tan, *Ultrason. Sonochem.*, 2014, **21**, 2069–2083.
27 T. Stepišnik Perdih, M. Zupanc and M. Dular, *Ultrason. Sonochem.*, 2019, **51**, 298–304.
28 E. Mousa, X. Hu, L. Ånnhagen, G. Ye, A. Cornelio, A. Fahimi, E. Bontempi, P. Frontera, C. Badenhorst and A. C. Santos, *Sustainability*, 2022, **15**, 15.
29 B. J. Ross, M. LeResche, D. Liu, J. L. Durham, E. U. Dahl and A. L. Lipson, *ACS Sustain. Chem. Eng.*, 2020, **8**, 12511–12515.
30 H. Y. Ting, T. Y. Wen, H. J. Yu and H. S. Chen, *J. Food Drug Anal.*, 2017, **25**, 16–26.
31 S. Chen, J. D. Wang, C. L. Chen and A. Mahmood, *Chem. Phys.*, 2020, **529**, 110466.
32 B. Li, X. H. Dou, K. Yu, N. Li, W. Zhang, H. J. Xu, Z. Q. Sun, Z. T. Wang and J. F. Wang, *J. Mol. Liq.*, 2021, **344**, 117875.
33 S. Sumitomo, M. Ueta, M. A. Uddin and Y. Kato, *Chem. Eng. Technol.*, 2019, **42**, 381–387.
34 M. J. Li, C. M. Liu, Y. B. Xie, H. B. Cao, H. Zhao and Y. Zhang, *Carbon*, 2014, **66**, 302–311.
35 J. N. Israelachvili, *Intermolecular and Surface Forces*, Academic press, 2011.
36 P. W. Atkins, J. De Paula and J. Keeler, *Atkins' Physical Chemistry*, Oxford university press, 2023.
37 M. F. Rabuni, *J. Appl. Sci. Process Eng.*, 2015, **2**, 30–43.
38 R. Golmohammadzadeh, Z. Dimachki, W. Bryant, J. Zhang, P. Biniaz, M. M. B. Holl, C. Pozo-Gonzalo and P. C. Banerjee, *J. Environ. Manage.*, 2023, **343**, 118205.
39 G. Z. Jiang, D. Lee, D. Raimbault, P. A. Anderson and G. A. Leeke, *Resour., Conserv. Recycl.*, 2024, **209**, 107778.